GCMS profiling and molecular docking of antioxidant compounds partially purified from *Ehretia laevis*

Vivek K.[1,2], Abdhul K.[1]*, Mahendran D.[3], Karthik S.[1] and Senthil Kumar V.[1]
1. PG and Research Department of Biotechnology, Nandha Arts and Science College (Autonomous), Erode – 638 052, Tamil Nadu, INDIA
2. PG and Research Department of Biotechnology, Sengunthar Arts and Science College (Autonomous), Tiruchengode, Namakkal – 637 205, Tamil Nadu, INDIA
3. Department of Biotechnology, Pavendar Bharathidasan College of Engineering and Technology, Tiruchirappalli - 620 024, Tamil Nadu, INDIA
*kabdhul@yahoo.com

Abstract

The present objective was to assess the phytochemical and in vitro antioxidant properties of Ehretia laevis ethyl acetate extract. Antioxidant activity was measured using the DPPH standard technique followed by purification using a solvent gradient based column and TLC. The DPPH positive fractions were analyzed using a gas chromatography technique. It was discovered that chloroform was more elute than hexane gradient in 22 distinct solvent gradient systems. Elution of fraction with hexane and water alone showed poor fractionation and no scavenging potential. Chloroform and methanol gradients gave maximum fractionation. Solvent chloroform/methanol at 1:1 ratio and at 3:7 ratio showed 74.6±1.15 66.6±1.17% DPPH free radical scavenging respectively. Fractions with Rf 0.64,0.73,0.82,0.9 cm exhibited strong free radical activity and their GCMS reveals presence of frequent novel compounds N-(t-butyl)-2-benzoylbenzamide, 1H-indolederivative, epoxycyclodecane-1-carboxylate, Naphtho[2,1-b]furan-6-carboxylic acid, 2(3H)-Furanone, 2-Fluoro-5-trifluoromethylbenzoic and isoquinolinone. In silico analysis reveals that the target having 5 active pockets were interacted with selected drug. The binding affinities of N'-acetyl-hydrazide ranged from −7.9 and 4-Fluoro-n-(2-methyl-1,3-dioxo-2,3-dihydro-1h-isoindol-5-yl)benzamide binding activity was -8.9kcal/mol.

According to the docked results, both compounds have the greatest affinity for the cancer target prptein and exhibit superior interaction with conserved catalytic residues. Additionally, ADMET experiments indicated that the phytochemicals' pharmacokinetics and toxicity characteristics were within acceptable bounds. According to the docked data, both compounds exhibit superior interaction with conserved catalytic residues and have the highest affinity for the epidermal growth factor. The presence of novel phytoconstituents' and their interaction ability promotes the traditional usage of E. laevis and offers crucial data for the development of cancer drugs.

Keywords: *E. laevis*, antioxidant, anticancer, benzoylbenzamide, hydrazide.

Introduction

Breast cancer is the most prevalent cancer among women with high mortality rates and has high global burden with approximately 4.4 million cases worldwide and about 411,000 deaths annually which represent 15% of the total cancers deaths. Currently available chemotherapeutics are associated with severe side effects, so discovery and development of novel and safe drugs from natural products is necessary[1]. Both endogenous and exogenous antioxidants can strengthen the immune system and can reduce the possibility of cancer because they function as "free radical scavengers", inhibiting and restoring injury brought on by ROS and RNS[17]. The demand for natural antioxidants in food and medicine has surged due to restrictions on synthetic antioxidants over health concerns such as carcinogenicity[9].

Numerous plant-derived compounds serve as free radical active oxygen scavengers helping to prevent chronic diseases[18]. Over 8,000 structural variations exist for the polyphenols, a class of plant chemicals. They have aromatic rings with hydroxyl groups[19]. India has historically relied on medicinal plants and their phytochemicals for health care and life enhancement.

In India resides the most extensive repository of conventional herbal plants and treatments. Ancient Indian life has long incorporated Ayurvedic, Unani and Siddha. Phytochemicals function as non-nutrient antioxidants by scavenging free radicals and neutralizing oxidative stress, a leading cause of chronic diseases[8]. *Ehretia laevis*, a small tree, is native to the tropical regions of Asia and Australia. 12 antioxidant compounds i.e. phenolic compounds were found to be in the extract of Ehretia species and exhibited substantial antioxidant potential[15].

The primary groups of polyphenols consist of phenolic acids, stilbenes, lignans and flavonoids. These antioxidants interrupt the free radical chain reaction by donating an electron and stabilizing the resulting complex[16]. *E. laevis* components have been reported for their wide-ranging uses including food, medicinal treatments for headaches, ulcers, spleen and lung disorders, astringent, anthelmintic, diuretic, demulcent and expectorant properties and ringworm therapy with a kernel oil and powder mixture[5]. The seeds possess anthelmintic properties according to Sharma et al[12].

The extract of *Ehretia laevis* Roxb might have important compounds as antioxidants and free radical scavengers, that could be related to liver protection medical use[14]. The

current study aimed to evaluate the phytochemical properties and *in vitro* antioxidant activities of *Ehretia laevis* ethyl acetate extracts.

Material and Methods

Plant extract preparation: The plant samples were collected in Perundurai, Tamil Nadu, India's Erode District. The collected *Ehretia laevis* plant was verified and authenticated. The leaves were carefully allowed to dry in the shade before being processed with a grinding machine into a fine powder. Next, a continuous Soxhlet extraction was performed on this coarse leaf powder. A porous thimble containing 100 grams of powdered material was used. 250 milliliters of ethylacetate served as the solvent. A round-bottom flask was connected to an isomantle-mounted Soxhlet extractor and condenser. The sample was extracted for six hours after the solvent was heated with an isomantle.

Column chromatography: The method of column chromatography was used to separate the phytoconstituents. A dried and clean glass column was employed for that. At 110°C, the silica gel mesh sizes #60-120 for column chromatography were activated. Without any air bubbles forming, a silica gel slurry made in water was poured into the column. After that, the stationary phase of silica gel was permitted to stabilize in the column. The extract was thoroughly mixed with the stationary phase and mobile phase to create the sample. After that, the solvent was removed to create a substance that flowed freely. In the column, this dried extract material was charged. The sample was eluted in gradient manner (22 solvent system) and fractions were collected. Solvent was recovered by simple distillation. Fractions giving same separation pattern on TLC plates were mixed together and forwarded for further studies.

TLC analysis: Thin layer chromatography (TLC) was used to evaluate the phytochemical components of the plant extract with aluminum-backed TLC plates (Merck, silica gel plates). In a nutshell, 1 mg/ml of the plant extract was reconstituted in ethyl acetate. Each extract concentration was spot-spotted in five microliters on TLC plates and then developed in distinct mobile systems, namely acetic acid (5:2:1:1), ethanol, chloroform and ethylacetate. Chromatogram development took place in a closed tank until the mobile phase passed through the adsorbent phase and reached the third of the plate. The plates were allowed to dry at room temperature, all of the compounds were examined at UV 365 nm to find out their R_f values.

DPPH assay: Ferric reducing capacity and DPPH scavenging potential (DPPH) were used to quantify each elute's antioxidant activity. In the DPPH scavenging assay, 25 minutes were given to the tubes after 1 mL of newly made DPPH solution (0.3 mM in methanol) was combined with 1 mL of extract (100 µg/mL). Without any extract, the reaction control was made in the same manner as before. At 515 nm, the absorbance was measured following incubation. The technique employed to quantify radical scavenging activity was the half-maximal inhibitory concentration (IC50). The following formula was used to determine the sample's capacity to scavenge the DPPH radicals.

Percentage of DPPH scavenging = Blank-test/blank x 100

Radical-scavenging activity by TLC-DPPH Method: The compounds having radical scavenging activity were identified *in situ* using the DPPH bioautography assay following separation on TLC plates. Using 0.2% DPPH in methanol, post-chromatographic treatment was performed. The plates' yellowish white or clearbands, which indicate antioxidant activity, were examined 10 minutes after DPPH derivatization and before DPPH.

Gas chromatography-mass spectroscopic analysis: The active TLC fractions were analyzed using a GC column (30 x 0.25 x 0.25 mm) and Shimadzu's GC-MS QP2010 series with electron impact ionization mode. The carrier gas (99.99%) utilized was helium gas, with an injection volume of 1 µL and a size ratio of 10:1 at a steady flow rate of 1 mL/min. The injector had approximately 250 °C in temperature and the ion source had 200 °C. The oven temperature increased by 15 °C each minute from 60°C to 280°C and it remained there for thirty minutes. The mass spectrophotometer was set up in positive electron ionization mode with an ionization energy of 70 eV and the solvent delay was varied between 0 and 45 minutes.

The components of the GC-MS equipment have been determined by matching with those found in the computer library (Willey and NIST) and the outcomes were tabulated.

Pharmacokinetics Parameters: The first step in evaluating a compound's potential as a therapeutic candidate is to ascertain its druggability. The druggability of the top phytochemicals was assessed using Swiss ADME. Pharmacokinetic and pharmacodynamic characteristics were evaluated with the aid of the AdmetSAR web server.

Preparation of Receptor Proteins and docking: The Protein Data Bank (https://www.rcsb.org/) provided three-dimensional (3D) structures of the epidermal growth factor receptor (EGFR; PDB ID: 3PP0) in the.pdb format for docking. The receptor proteins' binding pockets were calculated using the molecular computing environment program. The water atoms were removed, hydrogen atoms were added, any previously bound ligands were removed (if any). The protonation procedure was carried out and energy minimization was done in order to further adapt the receptor proteins for molecular docking. The molecular docking of ligands to the active amino acids of the binding pocket of the receptor proteins was done using the Autodock software. The relationships between the receptor proteins and important active substances were visualized using the UCSF chimera1.1 program.

Results and Discussion

Preliminary screening of DPPH active compounds: The extracted crude was first condensed on a silicon column and then eluted employing a gradient solvent technique consisting of hexane, chloroform, methanol and water. An extract eluted with a gradient of high polarity with low non-polar solvent showed substantial radical scavenging action against DPPH radicals. The *Rf* value of fractions eluted from the solvent system is given in table 1. Among the hexane chloroform, the ratio at 1:9 gave maximum fractions of five compared to hexane alone. Chloroform and methanol at 9:1 gave 9 different fractions, followed by 7 fractions by increasing methanol volume. Using four solvents 22 gradients, the separation was accomplished in gradient mode. Among them, hexane and water demonstrated an inadequate chemical separation.

It was reported that the extract yield in polar solvents (methanol 99%) was higher than in nonpolar hexane solvents and roughly equivalent to chloroform. TLC plate of an isolated compound sprayed with DPPH reveals that out of 22 gradients, 10 solvent systems have had antioxidant molecules. The *Rf* values of the fraction with antioxidant activity were 0.64, 0.73, 0.82 and 0.9 cm. Fraction with 0.9 cm R_f was isolated from a non-polar gradient containing hexane and chloroform and fraction 0.82 cm from methanol alone. Another two fractions were recovered from chloroform methanol gradient. It is possible to extract the bioactive component from natural materials using a variety of solvent systems. Ethyl acetate or methanol polar solvents were used in the extraction of hydrophilic substances.

Chloroform or hexane is used to extract more lipophilic substances. Chlorophyll and fatty acids can occasionally be extracted using hexane[2]. To assess the antioxidant activity of natural compounds, the test DPPH (2,2-diphenyl-1-picrylhydrazyl) was employed among 22 elutes and the fractions with maximum activity were represented on figure 1. The radical scavenging activity of 22 elutes was examined and compared against one another. Among the collected fractions, the solvent gradient system of B1, B2, C1, D1, D2, D5, D6, D7, D8 and E1 showed more than 50 % radical scavenging activity on the stable DPPH (Table 2). When reduced by hydrogen or electron donation, the color of the stable nitrogen-centered free radical, known as DPPH, transforms from violet to yellow. The compounds that can carry out this process, are categorized as radical scavengers or antioxidant.

Compared to the other fractions studied, D5 exhibited much superior radical scavenging activity (74.6±1.15) due to multiple fractions followed by D6 (61±1%) and D7(66.6±1.17%).

Table 1
***Rf* value of fraction eluted with two different silica mesh and its DPPH activity**

Code	Mobile phase	No. of visible fraction	*Rf* value cm	Antioxidant fraction R_f value
A1	Hexane	1	0.45	-
	Hexane chloroform			
B1	9:1	2	0.45,0.9	0.9
B2	8:2	2	0.45,0.9	0.9
B3	7:3	1	0.42	-
B4	6:4	1	0.28,0.32	-
B5	5:5	1	0.16	-
B6	4:6	2	0.6,0.62	-
B7	3:7	3	0.54, 0.56, 0.62	-
B8	2:8	4	0.54, 0.56, 0.62, 0.72	-
B9	1:9	5	0.25, 0.27, 0.32, 0.46, 0.48	-
C1	Chloroform	9	0.3,0.32,0.38,0.55,0.58, 0.62, 0.93	**0.73**
	Chloform-methanol			
D1	9:1	9	0.3,0.32,0.38,0.55,0.58, 0.62, 0.93	**0.73**
D2	8:2	4	0.31, 0.56,0.58, 0.64	0.64
D3	7:3	6	0.56,0.58, 0.6,0.64,0.66, 0.68	-
D4	6:4	3	0.45,0.48,0.54	-
D5	5:5	5	0.42, 0.48, 0.6, 0.64, 0.90	0.64, **0.82,** 0.90
D6	4:6	7	0.28, 0.4, 0.42, 0.48, 0.6, 0.64, 0.92	**0.82**
D7	3:7	7	0.23, 0.28, 0.4, 0.42, 0.6, 0.64, 0.72, 0.90	0.64, **0.82**
D8	2:8	5	0.20, 0.42, 0.64, 0.72, 0.90	**0.82**
D9	1:9	7	0.22, 0.26, 0.38, 0.40, 0.58, 0.60, 0.90	-
E1	Methanol	7	0.22, 0.26, 0.38, 0.40, 0.58, 0.90	**0.82**
F1	Water	1	0.3	-
Anti oxidant fractions				0.64,0.73,0.82,0.9

Table 2
Percentage of DPPH scavenging by column eluted fractions

Fraction	Percentage of free radical scavenging
B1	53.3333±0.57
B2	54.6±1.17
C1	58±1.7
D1	52±1
D2	59±1.15
D5	74.6±1.15
D6	61±1
D7	66.6±1.17
D8	59.3±1.15
E1	59.3±1.15

The percentage of free radical inhibition was represented in table 2. Presence of two extra fractions on D5 and D7 reflect a greater activity than D6. Rasika et al[10] have reported promising *in vitro* antioxidant activity of ethanol extract of leaves and stem of *Ehretia laevis* active against carbapenemase producing *Klebsiella pneumonia*.

GCMS analysis of antioxidant fractions: Figure 2 represents the GC spectrum. Fraction 1 reveals presence of 25 different peaks between RT 9.949 to 40.117 min. Cyclopentasiloxane was the first eluted compound and ethyl (1r*,2s*,11r*)-(+-)-3,10-dioxo-2,11-epoxycyclodecane-1-carboxylate was last eluted compound. Table 3 shows the list of compound matching with the peak of GCMS. Figure 3 shows GCMS of fraction 2 having 30 different peaks with 22 different compounds Cyclopentasiloxane, decamethyl (RT 9.94min 5.86%) was first identified compound and ethyl (1r*,2s*,11r*)-(+-)-3,10-dioxo-2,11-epoxycyclodecane-1-carboxylate (RT 40.205;0.14%) was the last eluted one (Table 4).

Compounds of fraction three shows 20 peaks with 15 different compounds between the times of 9.947 to 38.75min (Fig. 4). Cyclopentasiloxane, decamethyl-(RT 9.947; 0.82%) was the first eluted and silicone oil (RT 38.75; 3.49%) is the 20th peak identified.

Table 3
NIST library matched compounds of fraction 1

Peak	Retention time	Area %	Name
1	9.949	5.12	Cyclopentasiloxane, decamethyl-
2	13.867	14.36	Cyclohexasiloxane, dodecamethyl-
3	17.475	8.9	cycloheptasiloxane, tetradecamethyl-
4	20.707	5.68	benzoic acid, 2,4-bis(trimethylsiloxy)-, trimethylsilyl ester
5	23.5	3.52	Cyclohexasiloxane, dodecamethyl-
6	25.988	1.64	Silicate anion tetramer
7	28.257	1.41	Benzoic acid, 2,4-bis(trimethylsiloxy)-, trimethylsilyl ester
8	30.315	1.12	3,4-dihydroxymandelic acid-tetratms
9	32.22	1.05	Octasiloxane, 1,1,3,3,5,5,7,7,9,9,11,11,13,13,15,15-hexadecamethyl-
10	34.013	1.2	naphtho[2,1-b]furan-6-carboxylic acid, 3a-(1,3-dioxolan-2-yl)dodecahydro-2-hydroxy-6,9a-dimethyl-, methyl ester, [2r-(2.alpha.,
11	35.697	0.97	benzoic acid, 2,5-bis(trimethylsiloxy)-, trimethylsilyl ESTER
12	37.786	48.44	13-Docosenamide, (Z)-
13	38.012	0.07	Cyclopentanone, 2-(2-oxopropyl)-
14	38.841	0.19	1H-indole, 1-acetyl-3-[(1,2,3,6-tetrahydro-1-methyl-4-pyridinyl)carbonyl]-
15	38.873	0.21	1H-indole, 1-acetyl-3-[(1,2,3,6-tetrahydro-1-methyl-4-pyridinyl)carbonyl]-
16	38.959	0.57	4-Hydroxy-3-methylsulfanyl-4,5,6,7-tetrahydro-benzo[c]thiophene-1-carboxylic acid n'-acetyl-hydrazide
17	39.12	0.78	N-(t-butyl)-2-benzoylbenzamide
18	39.2	0.33	Ethyl (1r*,2s*,11r*)-(+-)-3,10-dioxo-2,11-epoxycyclodecane-1-carboxylate
19	39.35	0.22	N-(t-butyl)-2-benzoylbenzamide
20	39.519	0.1	14,19-DIoxoundecacyclo[9.9.0.0(1,5).0(2,12).0(2,18).0.(3,7).0(6,10).0(8,12).0(11,15).0(13,17).0(16,20)]icosane-4-syn,9-syn-dica
21	39.74	0.57	12-Azabicyclo(9.2.1)tetradeca-1(14)-ene-13-one
22	39.824	0.77	Ethyl (1r*,2s*,11r*)-(+-)-3,10-dioxo-2,11-epoxycyclodecane-1-carboxylate
23	39.995	1.48	N-(t-butyl)-2-benzoylbenzamide
24	40.052	0.54	N-(t-butyl)-2-benzoylbenzamide
25	40.117	0.76	Ethyl (1r*,2s*,11r*)-(+-)-3,10-dioxo-2,11-epoxycyclodecane-1-carboxylate

Table 4
NIST library matched compounds of fraction 2

Peak	Retention time	Area %	Name
1	9.94	5.86	Cyclopentasiloxane, decamethyl-
2	13.86	18.53	Cyclohexasiloxane, dodecamethyl-
3	17.47	10.95	Cycloheptasiloxane, tetradecamethyl-
4	20.70	6.78	Cyclooctasiloxane, hexadecamethyl-
5	23.5	5.1	1,3,3,3-Tetramethyldisiloxanyl tris(trimethylsilyl) orthosilicate #
6	25.986	2.93	2,2,4,4,6,6,8,8,10,10,12,12,14,14,16,16,18,18,20,20-icosamethylcyclodecasiloxane #
7	28.256	2.4	Benzoic acid, 2,4-bis(trimethylsiloxy)-, trimethylsilyl ester
8	30.313	2.37	Cyclononasiloxane, octadecamethyl-
9	32.217	2.1	2,2,4,4,6,6,8,8,10,10,12,12,14,14,16,16,18,18,20,20-Icosamethylcyclodecasiloxane #
10	33.047	0.32	Disulfide, dioctyl
11	34.011	2.08	2,2,4,4,6,6,8,8,10,10,12,12,14,14,16,16,18,18,20,20-icosamethylcyclodecasiloxane #
12	34.366	0.42	Octane
13	35.636	0.44	Octane
14	35.699	1.5	cyclononasiloxane, octadecamethyl-
15	36.857	0.28	disulfide, dioctyl
16	37.276	0.83	3,4-Dihydroxymandelic acid, 4TMS derivative
17	37.785	32.96	13-Docosenamide, (Z)-
18	37.975	0.12	Cyclopentanone, 2-(2-oxopropyl)-
19	38.044	1.03	Conhypoprotocetraric acid
20	38.767	0.86	3,4-Dihydroxymandelic acid, 4TMS derivative
21	38.875	0.23	N-(T-butyl)-2-benzoylbenzamide
22	39.505	0.28	N-(T-Butyl)-2-benzoylbenzamide
23	39.67	0.14	Ethyl (1r*,2s*,11r*)-(+-)-3,10-dioxo-2,11-epoxycyclodecane-1-carboxylate
24	39.68	0.09	1,2,3-TRI (T-Butyl)cyclopropenylium-hydrogene dichloride
25	39.941	0.22	14.Alpha.-fluoro-8-oxodes-a,b-cholestane
26	39.975	0.13	3-Phenylseleno acetic .gamma.-lactone
27	40.024	0.1	4,5,6,6A,10',11'-Hexahydrospiro{5'h-dibenzo[a,d]cycloheptene-5',3(3ah)-[4,5,6]methenocyclopentapyrazole}
28	40.055	0.16	1H-Furo[3,4-c]pyrrole-4-carboxylic acid, 6-(2-furanyl)hexahydro-1,3-dioxo-4-phenyl-, methyl ester, (3a.alpha.,4.beta.,6.beta.,6
29	40.12	0.66	Benzofuro[3,2-b]pyridine-1(2h)-carboxylic acid, 3-cyano-4-methyl-, ethyl ester
30	40.205	0.14	Ethyl (1r*,2s*,11r*)-(+-)-3,10-dioxo-2,11-epoxycyclodecane-1-carboxylate

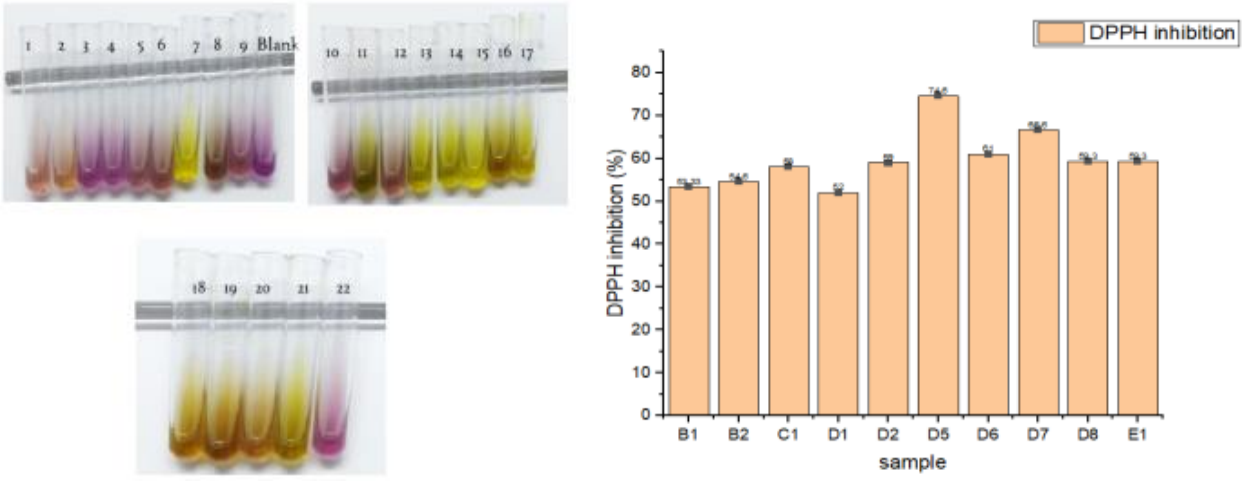

Figure 1: Percentage of DPPH scavenging by column eluted fractions

Table 5
NIST librarary matched compounds of fraction 3

Peak	Retention time	Area %	Name
1	9.947	0.82	Cyclopentasiloxane, decamethyl-
2	13.865	2.38	Cyclohexasiloxane, dodecamethyl-
3	17.473	1.47	Cycloheptasiloxane, tetradecamethyl-
4	20.706	0.74	Benzoic acid, 2,4-bis(trimethylsiloxy)-, trimethylsilyl ester
5	23.498	0.32	Cyclohexasiloxane, dodecamethyl-
6	25.987	0.15	Silicate anion tetramer
7	28.253	0.16	Benzoic acid, 2,6-bis(trimethylsiloxy)-, trimethylsilyl ester
8	30.312	0.15	3,4-Dihydroxymandelic acid-tetratms
9	32.218	0.2	2,2,4,4,6,6,8,8,10,10,12,12,14,14,16,16,18,18,20,20-icosamethylcyclodecasiloxane #
10	34.01	0.19	Naphtho[2,1-b]furan-6-carboxylic acid, 3a-(1,3-dioxolan-2-yl)dodecahydro-2-hydroxy-6,9a-dimethyl-, methyl ester, [2r-(2.alpha.,
11	37.37	0.05	Propane, 2,2-dimethyl-1-nitro-
12	37.445	0.67	2(3H)-Furanone, dihydro-5-tetradecyl-
13	37.638	0.32	Ethanone, 1-(3-methylenecyclopentyl)-
14	37.787	7.37	9-Octadecenamide, (Z)-
15	37.89	2.93	4-Fluoro-n-(2-methyl-1,3-dioxo-2,3-dihydro-1h-isoindol-5-YL)benzamide #
16	38.015	7.43	Dodecanoic acid, 1,2,3-propanetriyl ester
17	38.085	2.47	Glycine, n,n'-1,2-ethanediylbis[n-(2-butoxy-2-oxoethyl)-, dibutyl ester
18	38.41	39.94	Dodecanoic acid, 1,2,3-propanetriyl ester
19	38.523	28.75	Dodecanoic acid, 1,2,3-propanetriyl ester
20	38.75	3.49	Silicone oil

Table 6
NIST library matched compounds of fraction 4

Peak	Retention time	Area %	Name
1	9.949	4.32	Cyclopentasiloxane, decamethyl-
2	13.866	11.51	Cyclohexasiloxane, dodecamethyl-
3	17.472	6.64	Cycloheptasiloxane, tetradecamethyl-
4	20.708	3.39	Benzoic acid, 2,4-bis(trimethylsiloxy)-, trimethylsilyl ester
5	23.501	1.43	Cyclohexasiloxane, dodecamethyl-
6	25.987	0.68	1,3-Diphenyl-1-((trimethylsilyl)oxy)-1(z)-heptene
7	28.255	0.68	Benzoic acid, 2,6-bis(trimethylsiloxy)-, trimethylsilyl ester
8	30.313	0.59	Phosphonousdibromide, [2,2,2-trifluoro-1-(trifluoromethyl)-1-[(trimethylsilyl) oxy]ethyl]-
9	32.215	1.02	Naphtho[2,1-b]furan-6-carboxylic acid, 3a-(1,3-dioxolan-2-yl)dodecahydro-2-hydroxy-6,9a-dimethyl-, methyl ester, [2r-(2.alpha.,
10	34.01	1.17	Naphtho[2,1-b]furan-6-carboxylic acid, 3a-(1,3-dioxolan-2-yl)dodecahydro-2-hydroxy-6,9a-dimethyl-, methyl ester, [2r-(2.alpha.,
11	34.744	0.58	1,2-benzenedicarboxylic acid, dicyclohexyl ester
12	35.697	1.02	3,4-Dihydroxymandelic acid, 4TMS derivative
13	37.279	0.59	3,4-Dihydroxymandelic acid, 4TMS derivative
14	37.787	62.42	13-Docosenamide, (Z)-
15	38.64	0.24	14,19DioxoundecacyclO[9.9.0.0(1,5).0(2,12).0(2,18).0.(3,7).0(6,10).0(8,12).0 (11,15).0(13,17).0(16,20)]icosane-4-syn,9-syn-dica
16	38.7	0.54	2-Benzyl-3,4,4a,5,6,7-hexahydro--6-hydroxy-7-(1-pyrrolidinyl)-1(2h) isoquinolinone
17	38.785	1.29	Silane, [[4-[1,2-bis[(trimethylsilyl)oxy]ethyl]-1,2 phenylene]bis(oxy)] bis[trimethyl-
18	38.865	0.92	DL-3-O-Ethyl-2,6-di-o-benzyl-myo-inositol
19	38.9	0.49	2-Fluoro-5-trifluoromethylbenzoic acid, pentyl ester
20	38.95	0.45	14,19-Dioxoundecacyclo[9.9.0.0(1,5).0(2,12).0(2,18).0.(3,7).0(6,10).0(8,12).0(11,15).0 (13,17).0(16,20)]icosane-4-syn,9-syn-dica

Table 7
Kinase domain of Human EGF

CurPocket ID	Cavity volume (Å^3)	Center (x, y, z)	Cavity size (x, y, z)
C1	4502	9, 18, 23	27, 25, 17
C2	430	5, 38, 35	23, 11, 9
C3	312	22, 35, 27	12, 10, 6
C4	156	26, 21, 30	6, 9, 6
C5	149	15, 23, 12	7, 8, 6

Table 8
Binding affinity of N'-acetyl-hydrazide

CurPocket ID	Hydrogen bond		Score	Other interaction
	AA	Ligand		
C1	Thr862	O1	-7.9	Hpb:Lys, Leu, Thr, Val
C3	Asp 708 TYR835	O1	-6.2	HpB :Val,Tyr
	Val777(N0/N1)	O1		
C5	Thr 759(O/N) Leu 790 Thr 791	O1	-5	Hpb: Asp, Leu, Thr

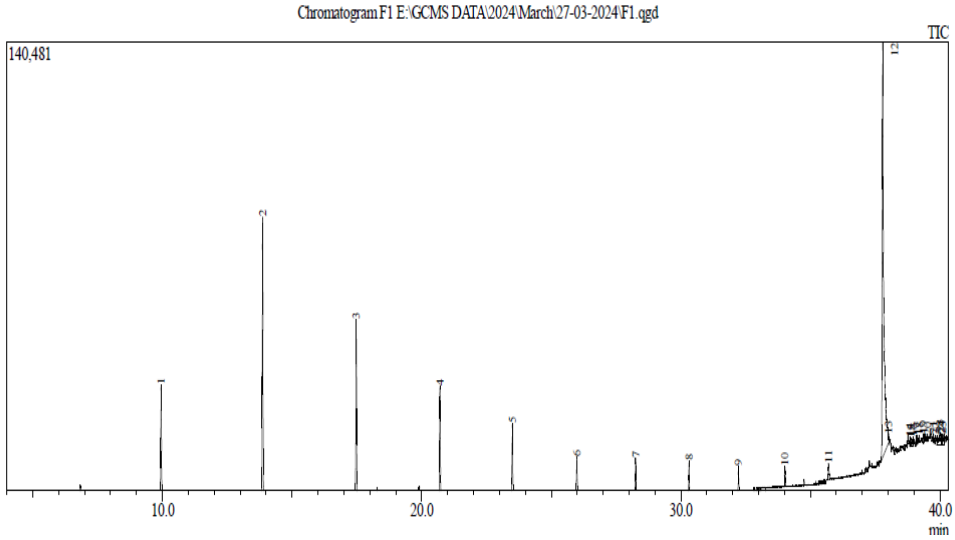

Figure 2: Gas chromatography mass spectrum of Fraction 1

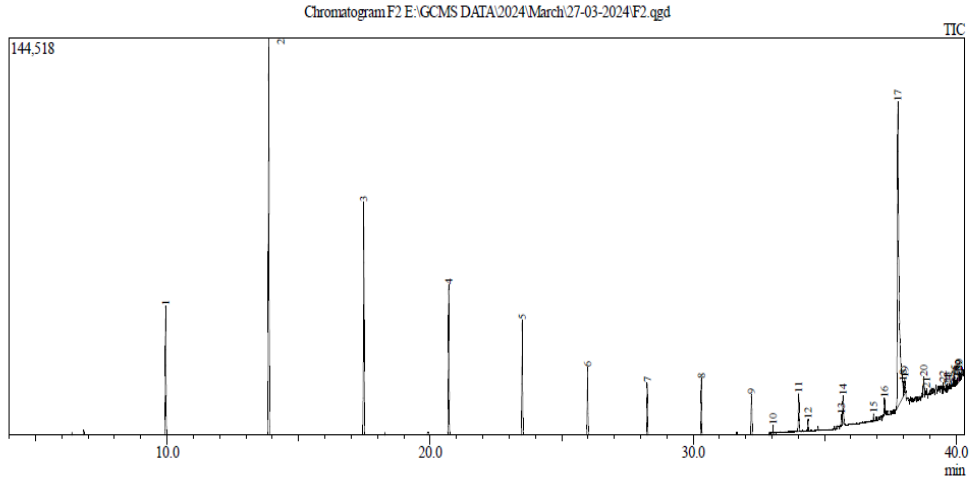

Figure 3: Gas chromatography mass spectrum of Fraction 2

Table 9
Binding score of 4-Fluoro-n-(2-methyl-1,3-dioxo-2,3-dihydro-1h-isoindol-5-yl)benzamide

Pocket	AA	Lig Atom	Score	Other interaction
C1	Arg 844 and 868	O1-NH2/NH1	-8.9	HP: LEU-Ala,Val,Thr, Asp,Phe
C3	Asn708	O1	-6.3	HP LEU-C1 WHB MET-C1
C4	Gln902 THR900	O1	-6.2	Cation pi ARG-C1

Table 10
ADMET property of selected compound

Properties	4-Fluoro-n-(2-methyl-1,3-dioxo-2,3-dihydro-1h-isoindol-5-yl)benzamide	4-Hydroxy-3-methylsulfanyl-4,5,6,7-tetrahydro-benzo[c]thiophene-1-carboxylic acid N'-acetyl-hydrazide
Molecular Weight (MW)	314.050	300.060
Volume	299.470	273.832
Density	1.049	1.096
nHA	5	5 (opt 0-12)
nHD	1	3 (opt 0-7)
TPSA	66.480	46.17 (opt 0-140)
logS	-3.48	-3.61 (opt -4 log mol/L)
logP	3.373	2.63 (opt 0-3)
logD	3.033	1.639(opt 1-3)
MDCK Permeability	1.9e-05	1.9e-05
Pgp-inhibitor	---	---
Pgp-substrate	---	---
HIA	---	---
F20%	---	--
F30%	---	+
PPB	91.855%	67.722%
VD	0.732	1.026
BBB Penetration	++	++
Fu	9.908%	47.979%
CYP1A2 inhibitor	++	---
CYP1A2 substrate	++	+
CYP2C19 inhibitor	+	--
CYP2C19 substrate	---	+
CL(ml/min/kg)	1.106	4.967(<5 low;>15 high)
T1/2	0.166	0.252
hERG Blockers	-	---
H-HT	--	+
DILI	+++	+++
AMES Toxicity	---	---
Rat Oral Acute Toxicity	--	---
FDAMDD	---	++
Skin Sensitization	--	-
Carcinogencity	--	+
Eye Corrosion	---	---
Eye Irritation	---	---
Respiratory Toxicity	---	--
Bioconcentration Factors	0.695	0.553
Acute Toxicity Rule	0 alert(s)	0 alert(s)
Genotoxic Carcinogenicity	1 alert(s)	1 alert(s)
Lipinski Rule	Accepted	Accepted

The probability values: 0-0.1(---), 0.1-0.3(--), 0.3-0.5(-), 0.5-0.7(+), 0.7-0.9(++) and 0.9-1.0(+++).

Nearly 76% of Dodecanoic acid, 7.37% of 9-Octadecenamide, (Z)- and 2.93% 4-Fluoro-n-(2-methyl-1,3-dioxo-2,3-dihydro-1h-isoindol-5-YL)benzamide are the major compounds detected from the fraction three (Table 5). Active compound fraction 4 GCMS given in figure 5 reveals 20 different peaks with cyclopentasiloxane, decamethyl (RT9.949) and 14,19-Dioxoundecacyclo [9.9.0.0(1,5). 0(2,12). 0(2,18). 0.(3,7).0(6,10). 0 (8,12). 0 (11,15).0 (13,17).0 (16,20)] icosane-4-syn,9-syn-dica (RT 38.95; 0.45%) as the last eluted compound.

Compound at RT 37.787 min was the most abundant compound identified as 13-Docosenamide, (Z) (62.42%) followed by 12.94 of cyclohexasiloxane, dodecamethyl (RT 13.8 min), cycloheptasiloxane (6.6%; RT17.472). In addition to that, catechol of 3,4-Dihydroxymandelic acid, isoquinolinone, carboxylic acid and benzoic acid derivatives and inositol were also identified (Table 6). Torane et al[15] have reported presence of 11 straight-chain alkanes like nonadecane, ddodecane and hexadecane from leaves of *Ehretia laevis*. Joshi et al[4] have reported presence of 13 different fattyacid methyl esters from the bark of *Ehretia laevis.* Our results were in contrast to the previous literature that stated presence of some unique novel compounds such as 1H-indole, 1-acetyl-3-[(1,2,3,6-tetrahydro-1-methyl-4-pyridinyl)carbonyl]-, ethyl (1r*,2s*,11r*)-(+-)-3,10-dioxo-2,11-epoxycyclodecane-1-carboxylate, N-(t-butyl)-2-benzoylbenzamide, Conhypoprotocetraric acid, cyclopropenylium-hydrogene dichloride, cholestane, 2(3H)-Furanone, dihydro-5-tetradecyl-, naphtho[2,1-b]furan-6-carboxylic acid, 2-Fluoro-5-trifluoromethylbenzoic acid, 4-Fluoro-n-(2-methyl-1,3-dioxo-2,3-dihydro-1h-isoindol-5-YL)benzamide. Most of the phytochemical identified in this study were not previously isolated or identified from this plant.

Molecular docking: Molecular docking studies were conducted to examine the crystal structure of EGF and the binding pattern of phytoconstituents from the plant *E. laevis*. The ligand's complex displayed the identical interaction profile as documented in previous studies. Tables 8 and 9 have the docking scores and binding energies of two chemical components that target EGF with interacted residues. Interaction of 4-Hydroxy-3-methylsulfanyl-4, 5, 6, 7-tetrahydro-benzo[c]thiophene-1-carboxylic acid N'-acetyl-hydrazide shows five different pockets from structure-based cavity detection (Table 8). Figure 6 shows the structure of the compound and its binding cavity on protein. The native ligand binds to receptor via hydrogen bonding with a binding energy of − 8.3 kcal/mol, where Thr 862 and Arg 849 represent the catalytic residues of C5.

TYR 835 and TYR 772 at pocket C2 are found as catalytic residues with a docking score of -6.2 kcal/mol (Fig. 7). It was noted that Lys, Leu, Thr, Val, Tyr and Asp residues take part in hydrophobic interaction with carbon atom of ligand.

Similarly, docking of 4-Fluoro-n-(2-methyl-1,3-dioxo-2,3-dihydro-1h-isoindol-5-yl)benzamide was performed and the binding cavity volume was given in table 9. The structure of 4-Fluoro-n-(2-methyl-1,3-dioxo-2,3-dihydro-1h-isoindol-5-yl)benzamide and its target cavity is given in figure 8.

Structure-based cavity detection reveals 5 pockets (Table 7) and template based cavity detection reveals two fit. The docked binding energy of the ligand is placed in the 3 cavities with docking scores of Arg 844 and 868 (C1), Asn708 (C3-6.6 kcal/mol) and Gln902 and Thr900 (C4-6.2kcal/mol). The cavities 1 and 3 showed a conformation on the formation of a conventional hydrophobic bond and C4 gave cation pi (Arg-C1). Because of the variety of biological functions that isoindole scaffolds and their associated molecules possess, they are highly significant.[3]

The binding affinities of N'-acetyl-hydrazide ranged from −7.9 to −5 kcal/mol with hydrophobic interaction. Benzamide derivatives have a docking score of -8.5 to 6.2 along with hydrogen bond, hydrophobic and cation interactions. From the docked results, it is evident that both compounds have displayed higher docking scores, stronger binding energies and better interaction with the conserved catalytic residues, leading to the inhibition of the associated signaling pathway in EGF.

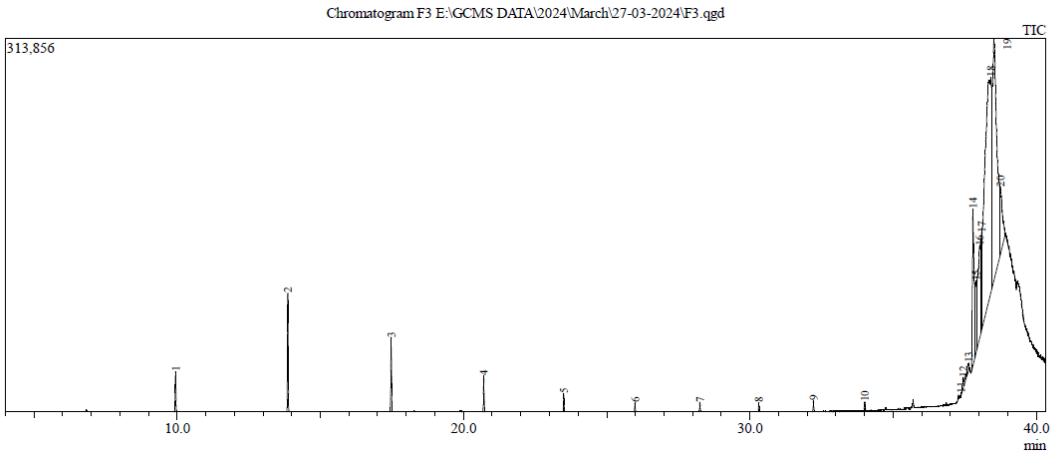

Figure 4: Gas chromatography mass spectrum of Fraction 3

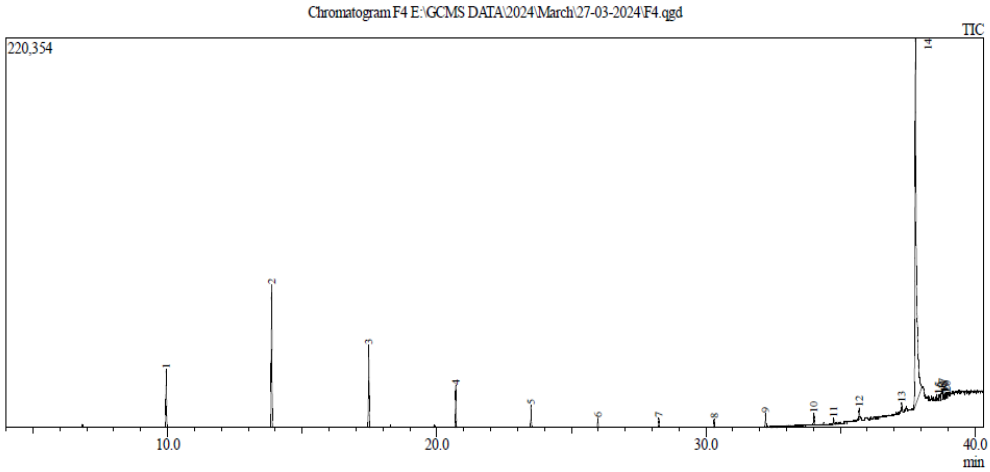

Figure 5: Gas chromatography mass spectrum of Fraction 4

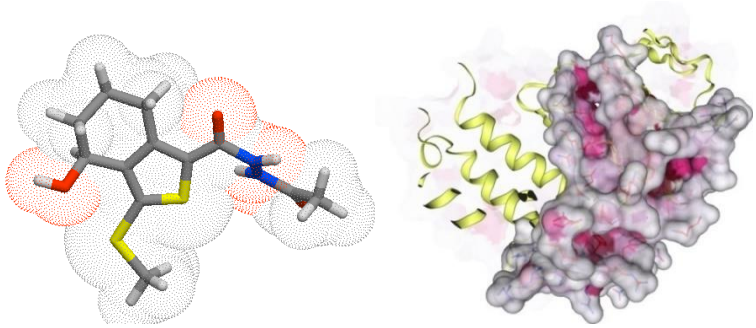

Figure 6: Structure of N'-acetyl-hydrazide and protein cavities

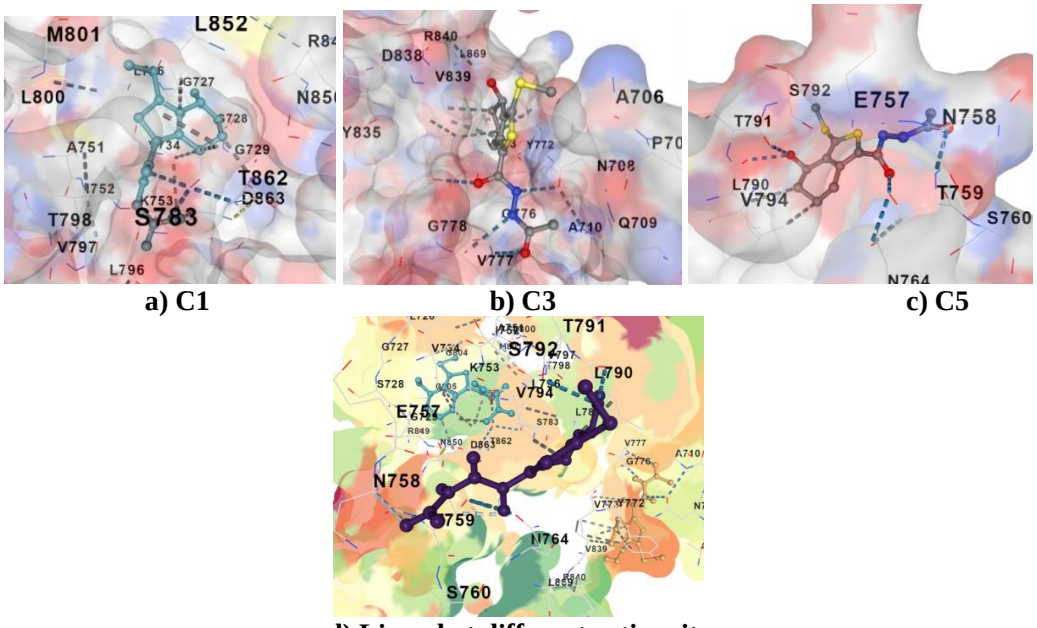

a) C1 **b) C3** **c) C5**

d) Ligand at different active site

Figure 7: Interaction of N'-acetyl-hydrazide and amino acid residues of target protein

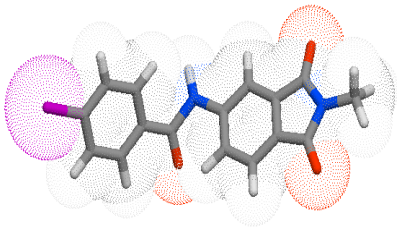

Figure 8: Structure of benzamide derivative

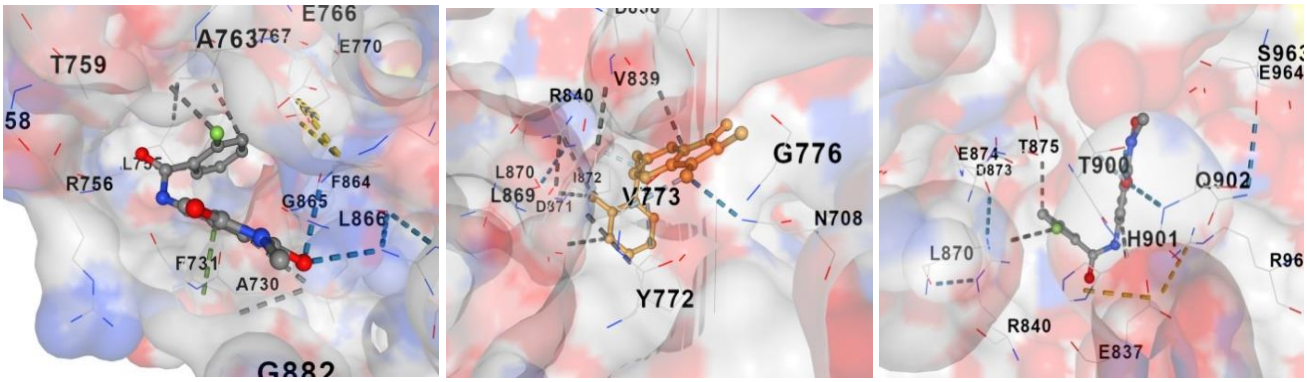

Figure 9: Interactions of ligands 4-Fluoro-n-(2-methyl-1,3-dioxo-2,3-dihydro-1h-isoindol-5-yl)benzamide with the binding site of EGFR

Pharmacokinetics and toxicity parameters of these phytochemicals were within acceptable limits according to ADMET studies. The carbonic anhydrases (CAs) inhibition by N-Acyl Hydrazones-derivative was reported by Küçükoğlu et al.[6]

ADME properties: Selected ligands followed the Lipinski rule, TPSA parameter and P-glycoprotein non-inhibition, thereby showing good intestinal absorption and an acceptable range of BBB values (Table 9). Both the compounds showed aqueous solubility values within the range; it was predicted that the selected ligands do not show AMES toxicity, hepatotoxicity, or skin sensitivity. In addition, it did not inhibit hERG-I (low risk of cardiac toxicity). The fraction of unbound plasma for benzamide is low with poor bioavailability and no carcinogenicity. Both were negative on AMES and acute toxcarcinogenic and bioavailability (F30+), less carcinogenic, negative on Pgp substrate. Both were negative on AMES and acute toxicity. 4-Fluoro-n-(2-methyl-1,3-dioxo-2,3-dihydro-1h-isoindol-5-yl)benzamide was found to be a CYP1A2 inhibitor (Fig. 9). Both compounds have a probability of CYP1A2 substrate.

The absorption potential and lipophilicity are characterized by Log P and LogS respectively. For better penetration of a drug molecule into a cell membrane, the TPSA should be less than 140 Å. However, the value of Log P differs based on the drug target. The ideal Log P value for oral and intestinal absorption is 1.35 − 1.80; the aqueous solubility of ligands is ideally optimum at -4 log mol/L while the blood brain barrier (BBB) value ranges between −3.0 and 1.2. In addition, non-substrate P-glycoprotein causes drug resistance. Isolation of novel compounds from *Ehretia* laevis was very scare. Subhash et al[13] reported the *in silico* prediction of *Ehretia laevis* phytochemical targeting TNF-α-associated signaling pathway.

Conclusion

This study demonstrated that *E. leavis* is potent novel phytochemical can be partially purified by solvent gradient system. It showed anticancer properties with strong antioxidant and inhibitory effects against epidermal growth factor receptor.

Acknowledgement

The authors are thankful to the Management of Nandha Arts and Science College for extending facilities and necessary support.

References

1. Ayaz M., Ullah F., Sadiq A., Kim M.O. and Ali T., Natural products-based drugs: potential therapeutics against Alzheimer's disease and other neurological disorders, *Front Pharmacol.*, **10**, 1417 **(2019)**

2. Cosa P., Vlietinck A.J., Berghe D.V. and Maes L., Anti-infective potential of natural products: How to develop a stronger *in vitro* 'proof-of-concept', *J Ethnopharmacol*., **106**, 290–302 **(2006)**

3. Ferenc Csende and Andrea Porkoláb, Antiviral activity of isoindole derivatives, *J. Med. Chem. Sci*, **3**, 254-285 **(2020)**

4. Joshi U.P. and Wagh R.D., GC-MS analysis of phytochemical compounds present in the bark extracts of *Ehretia laevis* Roxb., *Int. J. Res. Dev. Pharm. Life Sci*, **7**, 3150–3154 **(2018)**

5. Jyothirmai N., Nagaraju B., Yasodeepika M., Suresh Kumar J. and Rani S.G., Evaluation of Anti-Inflammatory and Anti-Bacterial Activities of Different Solvent Extracts of *Ehretia laevis* Roxb., *J. Pharm. Sci. & Res.*, **8(8)**, 715-720 **(2016)**

6. Küçükoğlu K., Çevik U.A., Nadaroglu H., Celik I., Işık A., Bostancı H.E., Özkay Y. and Kaplancıklı Z.A., Synthesis and Molecular Docking of New N-Acyl Hydrazones- Benzimidazole as hCA I and II Inhibitors, *Med Chem*, **19(5)**, 485-494 **(2023)**

7. Oselusi S.O., Sibuyi N.R.S., Meyer M. and Madiehe A.M., Ehretia Species Phytoconstituents as Potential Lead Compounds against *Klebsiella pneumoniae* Carbapenemase: A Computational Approach, *Biomed Res Int*, **12**, 8022356 **(2023)**

8. Pandey M.M., Rastogi S. and Rawat A.K., Indian traditional ayurvedic system of medicine and nutritional supplementation, *Evid Based Complement Alternat Med*, **2013**, 376327 **(2013)**

9. Pham-Huy L.A., He H. and Pham-Huy C., Free radicals, antioxidants in disease and health, *Int J Biomed Sci*, **4(2)**, 89-96 **(2008)**

10. Rasika C.T., Adsul Vaishali B., Shendkar Chandrakant D. and Deshpande Nirmala R., Evaluation of *In Vitro* Nitric Oxide

Scavenging Activity of Medicinal Plant- *Ehretia laevis*. *Asian J. Research Chem*,**4(12),**1864-1866 **(2011**)

11. Sharma B., Gupta S. and Sharma K., Natural folk remedy for menorrhagia, *Journal of Information, Knowledge and Research in Humanities and Social Service*, **2(1)**, 86-88 **(2011)**

12. Sharma P., Shri R., Ntie-Kang F. and Kumar S., Phytochemical and Ethnopharmacological Perspectives of *Ehretia laevis*, *Molecules*, **26(12)**, 3489 **(2021)**

13. Subhash R.Y., Shah Sapan K., Arora Sumit K., Moharir Keshav S. and Lohiya Govind K., *In silico* prediction of phytoconstituents from *Ehretia laevis* targeting TNF-α in arthritis, *Digital Chinese Medicine*, **4(3)**, 180-190 **(2021)**

14. Tarke Santosh Rangnathrao and Shanmugasundaram P., Antioxidant and Hepatoprotective activity of *Ehretia laevis* Roxb against paracetamol induced acute Hepato toxicity in wistar rats, *Res. J. Pharm. and Tech*, **12(12)**, 6143-6148 **(2019)**

15. Torane R.C., Kamble G.S., Gadkari T.V., Tambe A.S. and Deshpande N.R., GC-MS study of nutritious leaves of *Ehretia laevis*, *Int. J. Chem. Res*, **3**, 1589–1591 **(2011)**

16. Tsao R. and Deng Z., Separation procedures for naturally occurring antioxidant phytochemicals, *J Chromatogr B*, **812**, 85–99 **(2004)**

17. Valko M. et al, Free radicals, metals and antioxidants in oxidative stress-induced cancer Mini-review, *Chem. Biol. Interact*, **160**, 1–40 **(2006)**

18. Willcox J.K., Ash S.L. and Catignani G.L., Antioxidants and prevention of chronic disease. Review, *Crit. Rev. Food. Sci. Nutr*, **44**, 275–295 **(2004)**

19. Wu W., Li G., Zhou W., Wang E., Zhao X., Song X. and Zhao Y., Comparison of Composition, Free-Radical-Scavenging Capacity and Antibiosis of Fresh and Dry Leave Aqueous Extract from *Michelia shiluensis*, *Molecules*, **28(16)**, 5935 **(2023)**.

(Received 04th June 2024, accepted 08th August 2024)